International Journal of Multidisciplinary Research and Modern Education (IJMRME)
ISSN (Online): 2454 - 6119
(www.rdmodernresearch.com) Volume II, Issue II, 2016

PERFORMANCE ANALYSIS OF AN DUAL VOLTAGE SOURCE INVERTER WITH ENHANCED CONTROL SCHEME FOR GRID CONNECTED APPLICATIONS

M. Chandini*, P. V. Prasuna & Ch. V. Pujitha*****
* PG Scholar, Department of Electrical and Electronics Engineering, Pragati Engineering College, Surampalem, Andhra Pradesh
** Associate Professor, Department of Electrical and Electronics Engineering, Pragati Engineering College, Surampalem, Andhra Pradesh
*** Assistant Professor, Department of Electrical and Electronics Engineering, Pragati Engineering College, Surampalem, Andhra Pradesh

Abstract:
This paper presents a dual voltage source inverter (DVSI) scheme to enhance the power quality and reliability of the micro grid system. The proposed scheme is comprised of two inverters, which enables the micro grid to exchange power generated by the distributed energy resources (DERs) and also to compensate the local unbalanced and nonlinear load. The proposed current controller is designed in the synchronous reference frame and composed of a proportional–integral (PI) controller and a repetitive controller (RC) with PWM generator. An RC serves as a bank of resonant controllers, which can compensate a large number of harmonic components with a simple delay function. Hence, the control strategy can be greatly simplified. Therefore, the proposed control method can be easily adopted into the traditional DG control system without installation of extra components. Despite the reduced number of sensors, the grid current quality is significantly improved compared with the traditional methods Hysteresis with the PI controller. The operation principle of the proposed control method is analyzed in detail, and its effectiveness is validated through simulated on MATLAB/Simulink software.

Key Words: Dual Voltage Source Inverter, Micro Grid, PI Controller, Resonant Controller & THD.

1. Introduction:

Several compensation methods have been implemented in order to avoid the grid current quality problems [1]. A novel compensation technique has been introduced to nullify the THD of the grid current under distorted voltage. The harmonic components are extracted from the grid voltage by using this method. In order maintain the quality grid current, the grid voltage harmonic components should not be varied. To reduce the effect of fifth and seventh harmonic grid voltages on grid current resonant controller is tuned at sixth multiple of fundamental frequency harmonic grid voltages on the grid current quality by using resonant controllers the quality of the grid current is improved. More resonant controllers should be used if we considered higher order components as a single resonant controller can compensate only one specific harmonic component. But complexity of the control system increases by adding more controllers. A repetitive control technique was introduced to improve the voltage or current quality of the system. A repetitive controller (RC) serves as a bank of resonant controllers and compensates large number of harmonic components with a simple delay structure. There will be negative impact on grid current quality due to the presence of grid voltage distortion and nonlinear loads in DG local load. So an advanced current control strategy for the grid connected DG was introduced, to eliminate the effect of grid voltage distortion and nonlinear load effect.

A Dual Voltage Source Inverter (DVSI) scheme is introduced .Main Voltage Source Inverter (MVSI) is used to inject real power generated by micro grid and Auxiliary Voltage Source Inverter (AVSI) is used to compensate unbalanced load and reactive harmonics. If at the dc there is sufficient renewable power is available then rated capacity of MVSI is used to inject real power to the grid. The Fundamental positive sequence of currents has to be tracked by the inverter as real power is supplied by main inverter, which reduces the main inverter band width requirement. The inverter used here consists of two separate dc links. As zero sequence of load current are supplied by AVSI, a three-phase three-leg inverter topology with a single dc storage capacitor can be used for the main inverter, which reduced the main inverter dc link voltage. Hence there will be increase in reliability, less band width requirement of main inverter, better utilization of micro grid power and filter size get reduces by using DVSI which consists of two inverters. [2-3].

2. Dual Voltage Source Inverter:

A. System Topology:

Figure 1 represents a proposed DVSI topology with a neutral point clamped (NPC) inverter to realize AVSI and a three-leg inverter for MVSI [4]. They supply a nonlinear and unbalanced load at PCC connected to the grid. In the load current the reactive, harmonics, and unbalance components are compensated by AVSI. i_a, i_b, and i_c represents load currents in three phases respectively. Also $i_{g(abc)}$, $i_{\mu m(abc)}$, $i_{\mu gx(abc)}$ represents grid currents, MVSI currents, and AVSI currents in three phases, respectively. A split capacitor topology is used by AVSI with two capacitors C1 andC2 of the dc link. The power available at distributed energy resource is delivered by MVSI to grid.

The DER can be a dc source or an ac source with rectifier coupled to dc link. Generally nonconventional al energy sources such as photovoltaic and fossil fuels are generates a low dc power, while the variable ac voltages are generated from the wind turbine. Hence before connecting it to the input of MVSI a power condition stage is should be used. Here DER used as a DC source and to eliminate high frequency switching component an inductor filter used. Feeder resistance Rg and inductance Lg are assumed. The PCC voltages effected due to the feeder impedance. Section III describes the extraction of fundamental positive sequence of PCC voltages and control.

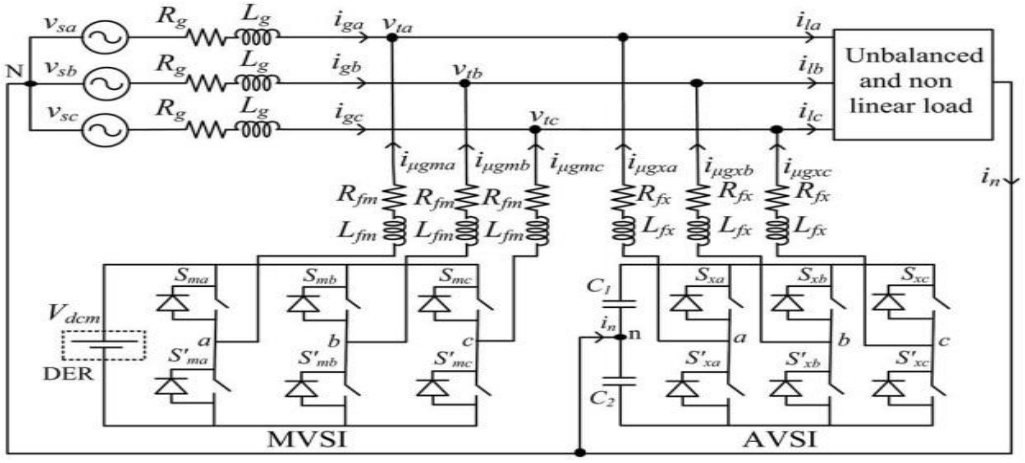

Figure 1: Strategy for the reference current generation of two inverters in DVSI scheme.

B. Design of DVSI Parameters:

AVSI: The AVSI parameters are like dc-link voltage (V_{dc}), dc storage capacitors (c_1 andc_2), interfacing inductance (L_{fx}), and hysteresis band ($\pm h_x$).The dc-link voltage across

each capacitor is taken as 1.6 times the peak of phase voltage. The total dc-link voltage reference (V_{dcref}) is found to be 1040 V. Values of dc capacitors of AVSI are chosen based on the change in dc-link voltage during transients. Let total load rating is S kVA.

In certain condition like drastic variation in the voltages or power the load power varies from the minimum to the maximum i.e., 0 to SkVA. To maintain load power demand exchange of real power should be needed during transients, which will results i the deviation of the capacitor voltage from its reference voltage. Let the voltage controller takes n cycles, i.e., nT seconds to act, where T is the system time period. During transients AVSI exchange minimum energy i.e., nST. Which is equal to change in capacitor stored energy. Therefore

$$\frac{1}{2}C_1(V_{dcr}^2 - V_{dc1}^2) = nST \quad (1)$$

Where, V_{dcr} and $V_{dc1}$are the reference dc voltage and maximum permissible dc voltage across c_1 during transient, respectively. Here, S = 5 kVA, V_{dcr} = 520 V, V_{dc1}= 0.8 $*V_{dcr}$ or 1.2 $*V_{dcr}$, n = 1, and T = 0.02 s. Substituting these values in (1), the dc link capacitance (c_1) is calculated to be 2000 μF. Same value of capacitance is selected for c_2. The interfacing inductance is given by

$$L_{fx} = \frac{1.6V_m}{4h_x f_{max}} \quad (2)$$

Assuming a maximum switching frequency (f_{max}) of 10 kHz and hysteresis band (h_x) as 5% of load current (0.5 A), the value of $L_{fx}$is calculated to be 26mH.

MVSI: A three leg inverter scheme is used by MVSI. Its dc-link voltage is obtained as 1.15 $*V_{ml}$, where V_{ml} is the peak value of line voltage. This is calculated to be 648 V. At unity power factor balanced sinusoidal current is obtained by MVSI. Hence MVSI is free from Zero sequence switching harmonics. Compared to the AVSI, MVSI doesn't require any filter [5]. In this analysis, a filter inductance (L_{fm}) of 5mH is used.

3. Control Strategy for DVSI Scheme:

A. Instantaneous Symmetrical Component Theory (ISCT):

For unbalanced and nonlinear load compensations ISCT was developed primarily by active power filters. The system topology shown in Fig. 2 is used for realizing the reference current for the compensator [6]. The ISCT for load compensation is derived based on the following three conditions

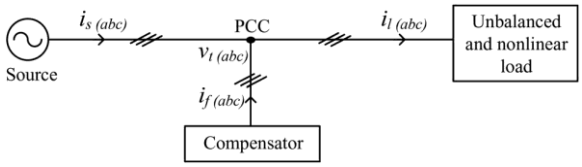

Figure 2: Schematic diagram of an unbalanced and nonlinear load compensation scheme

The source neutral current must be zero. Therefore

$$i_{sa} + i_{sb} + i_{sc} = 0 \quad (3)$$

The phase angle between the fundamental positive sequence voltage ($\angle V_{ta1}^{+}$) and source current (i_{sa}) is φ

$$\angle v_{ta1}^{+} = \angle i_{sa} + \varphi \quad (4)$$

The average real power of the load (P_1) should be supplied by the source

$$v_{ta1}^{+} i_{sa} + v_{tb1}^{+i} i_{sb} + v_{tc1}^{+} = P_l \quad (5)$$

Solving the above three equations, the reference source currents can be obtained as

$$i^*_{sa} = \left(\frac{v^+_{ta1} + \beta(v^+_{tb1} - v^+_{tc1}}{\sum_{j=a,b,c} v^{+2}_{tj}} \right) P_l$$

$$i^*_{sb} = \left(\frac{v^+_{tb1} + \beta(v^+_{tc1} - v^+_{ta1}}{\sum_{j=a,b,c} v^{+2}_{tj}} \right) P_l \qquad (6)$$

$$i^*_{sc} = \left(\frac{v^+_{tc1} + \beta(v^+_{ta1} - v^+_{tb1}}{\sum_{j=a,b,c} v^{+2}_{tj}} \right) P_l$$

Where β = tan√ φ 3. The term φ represents the phase angle between source current and fundamental positive sequence of positive sequence of PCC voltage and source current. For source current to be unity, substitute β = 0 in (6). Thus, the reference source currents for three phases are given by

$$i^*_{s(abc)} = \left(\frac{v^+_{t(abc)1}}{\sum_{j=a,b,c} v^{+2}_{tj}} \right) P_l \qquad (7)$$

Where i_{sa}^*,i_{sb}^*, $i_{sc}^*$and are fundamental positive sequence of load currents drawn from the source, when it is supplying an average load power P_l. The power $P_l$can be computed using a moving average filter with a window of one-cycle data points as given below

$$P_l = \frac{1}{T} \int_{t_1 - T}^{t_1} \left(v^+_{ta1} i_{la} + v^+_{tb1} i_{lb} + v^+_{tc1} i_{lc} \right) dt \qquad (8)$$

Where, $t_1$is any arbitrary time instant. Finally, the reference currents for the compensator can be generated as follows:

$$i^*_{f(abc)} = i_{l(abc)} - i^*_{s(abc)} \qquad (9)$$

Equation (9) can be used to generate the reference filter currents using ISCT, when compensation of load is performed by single inverter, the source supplies the active power needed. The control algorithm should be modified when it is used for DVSI. The source currents $i_{s(abc)}$ and filter currents $i_{f(abc)}$ will be replaced as grid currents $i_{g(abc)}$and AVSI currents $i_{\mu gx(abc)}$ respectively, in further sections.

B. Control Strategy of DVSI:

Control strategy of DVSI is developed in such a way that grid and MVSI together share the active load power, and AVSI supplies rest of the power components demanded by the load.

Reference Current Generation for Auxiliary Inverter:

A constant dc link voltage should be maintained to operate AVSI properly. But variation occurs due to switching and ohmic losses. These losses termed as P_{loss} should also be supplied by the grid. P_{loss} is derived on the condition that average dc capacitor current is zero to maintain a constant capacitor voltage [6]. A PI controller is used to generate P_{loss} term as given by

$$P_{loss} = K_{Pv} e_{vdc} + K_{Iv} \int e_{vdc} dt \qquad (10)$$

Where, $e_{vdc} = v_{dcref} - v_{dc}$, v_{dc} represents the actual voltage sensed and updated per cycle. In the above equation, K_{Pv} and K_{Iv} represent the proportional and integral gains of

dc-link PI controller, respectively. The P_{loss} term thus obtained should be supplied by the grid, and therefore AVSI reference currents can be obtained as given in (11).

$$i^{*}_{\mu gxa} = i_{la} - \left(\frac{v^{+}_{ta1}}{\sum_{j=a,b,c} v^{+2}_{tj}}\right)(P_l + P_{loss})$$
$$i^{*}_{\mu gxb} = i_{lb} - \left(\frac{v^{+}_{tb1}}{\sum_{j=a,b,c} v^{+2}_{tj}}\right)(P_l + P_{loss}) \qquad (11)$$
$$i^{*}_{\mu gxc} = i_{lc} - \left(\frac{v^{+}_{tc1}}{\sum_{j=a,b,c} v^{+2}_{tj}}\right)(P_l + P_{loss})$$

Reference Current Generation for Main Inverter:

A balanced sinusoidal current are supplied from MVSI by using available renewable power at DER. By neglecting MVSI losses power injected to grid will be equal to that available power at DER ($P_{\mu g}$).The following equation generates MVSI reference currents for three phases (a, b, and c)

$$i^{*}_{\mu gm(abc)} = \left(\frac{v^{+}_{ta1}}{\sum_{j=a,b,c} v^{+2}_{tj}}\right)P_{\mu g} \qquad (12)$$

Where, $P_{\mu g}$is the available power at the dc link of MVSI.

The reference currents obtained from (11) to (12) are tracked by using PWM current controller.

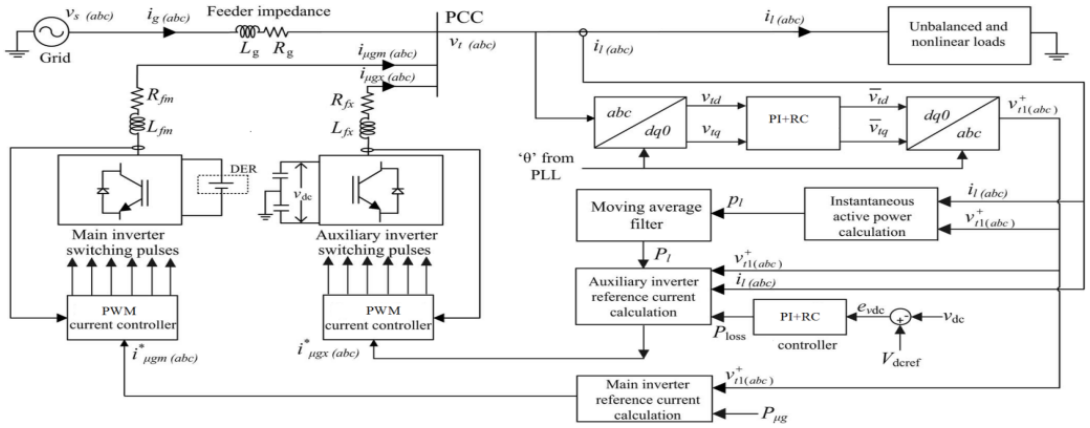

Figure 3: Control diagram of Dual VSI

Also a first-order inductor filter, is used in the proposed DVSI scheme which retains the closed-loop system stability [7-11]. The entire control strategy is schematically represented in Fig.3. Applying Kirchoff's current law (KCL) at the PCC in figure 3

$$i_{\mu gxj} = i_{lj} - (i_{gj} + i_{\mu gmj}) \text{ for j=a,b,c} \qquad (13)$$

By using (11) and (13), an expression for reference grid current in phase-a (i_{ga}^{*}) can be obtained as

$$i^{*}_{ga} = \left(\frac{v^{+}_{ta1}}{\sum_{j=a,b,c} v^{+2}_{tj}}\right)\left[(P_l + P_{loss}) - P_{\mu g}\right] \qquad (14)$$

It can be observed that, if the quantity (P_l + P_{loss}) is greater than $P_{\mu g}$, the term

[(P_l + P_{loss}) – $P_{\mu g}$]will be a positive quantity, and i_{ga}^* will be in phase with V_{ta1}^*. This operation can be called as the grid supporting or grid sharing mode, as the total load power demand is shared between the main inverter and the grid. The term, P_{loss} is usually very small compared to P_1. On the other hand, If(P_l + P_{loss}) is less than $P_{\mu g}$ then [(P_l + P_{loss}) – $P_{\mu g}$)] will be a negative quantity, and hence i_{ga}^*will be in phase opposition with V_{ta1}^*. This mode of operation is called the grid injecting mode, as the excess power is injected to grid.

Resonant Controller (RC):

An advanced current controller is proposed by using a PI with an RC in the d–q reference frame. The block diagram of the current controller is shown in Fig. 4. The open-loop transfer function of the PI and RC in a discrete-time domain is given respectively in

$$G_{PI}(z) = K_p + \frac{K_i z}{z-1} \qquad (15)$$

$$G_{RC}(z) = \frac{K_r z^k z^{-N/6}}{1 - Q(z) z^{-N/6}} \qquad (16)$$

The harmonic currents in the grid current are eliminated through RC. Meanwhile, the significant of the PI controller is to improve the dynamic response of the grid current and to stabilize the whole control system.

The number of delay samples of the RC given in (16) is N/6, where $N=f_{Sample}/ f_s$ is the number of samples in one fundamental period, which is defined as the ratio of the sampling frequency and the fundamental frequency of system (f_s). In fact, the conventional RC can be utilizes to reduce the harmonic components but it gives the slow dynamic response due to more delay time by N samples which is the main disadvantage of traditional RC. To remove the delay problem of the traditional RC, we consider only the (6n±1)th (n=1,2,3...) harmonics because they are dominant components in three-phase systems. The time delay of the RC in [13] is thereby reduced six times compared with the traditional one as N/6.An versatile controlling is proposed to improvise the grid frequency variations. Nevertheless, the current controller needs some additional components, such as filters and controllers, to implement the frequency adaptive controllers.

In this paper, the current controller is designed in such a way that it can control both the current harmonic and the grid frequency variation, simultaneously. When the grid frequency varies, the grid frequency (f_s) is quickly detected by the PLL, and the frequency variation is compensated directly by adjusting the number of delay samples,

$$\text{i.e., } N/6 = N = \frac{f_{sample}}{f_s}$$

Design of RC:

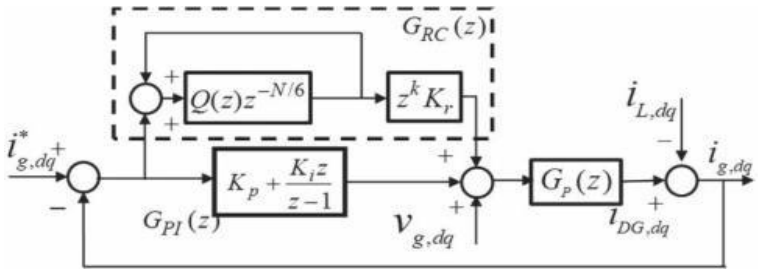

Figure 4: Schematic diagram of Resonant controller

The RC has three main components that must be determined: the filter Q(z), the phase lead term z^k, and the RC controller gain Kr. Selection of the Filter Q(z): Q(z) is used to improve the system stability by reducing the peak gain of the RC at a high-frequency range. There are two methods that have been commonly used to select Q(z): a closed unity gain Q(z)=0.95 and a zero phase-shift LPF Q(z)=(z+2+z−1)/4. In this paper, we use Q(z)=(z+2+z−1)/4 because it gives the high peak gain of the PI-RC at the low-frequency range and low peak gain (less than 0 dB) at the high-frequency range (higher than 2 kHz). The system stability will be improved by using the low peak gain at the high-frequency range can effectively prevent the system unstable.

Determination of the Phase Lead Term z^k Since the control plant $G_p(z)$i.e., the LC filter, acts as an LPF, which introduces some phase lag, the phase lead term z^k is required to compensate the phase lag of $G_p(z)$ and k is selected to minimize the phase displacement of $G_p(z)$ z^k, Determination of the Controller Gain K_r : To determine controller gain, the magnitude response of the PI-RC is investigated. The proposed controller PI-RC provides different values of Kr for getting the different frequency responses, As K_r value reduces by reducing the peak gain of the RC at the resonant frequency. With K_r =0.1or

K_r =0.25, the peak gains of the PI-RC are too small; therefore, it is not adequate to offer good steady-state performance for harmonic current compensation. Meanwhile, with K_r =1, the PI-RC has high peaks up to 2 kHz, and it is sufficient to compensate harmonics up to the 39th order. Therefore, we select K_r =1.

4. Simulation Studies and Discussion:

The simulation model of DVSI scheme shown in Fig. 5 is developed in MATLAB/Simulink to evaluate the performance. The simulation parameters of the system are given in Table 1. The simulation study demonstrates the grid sharing and grid injecting modes of operation of DVSI scheme in steady state as well as in transient conditions.

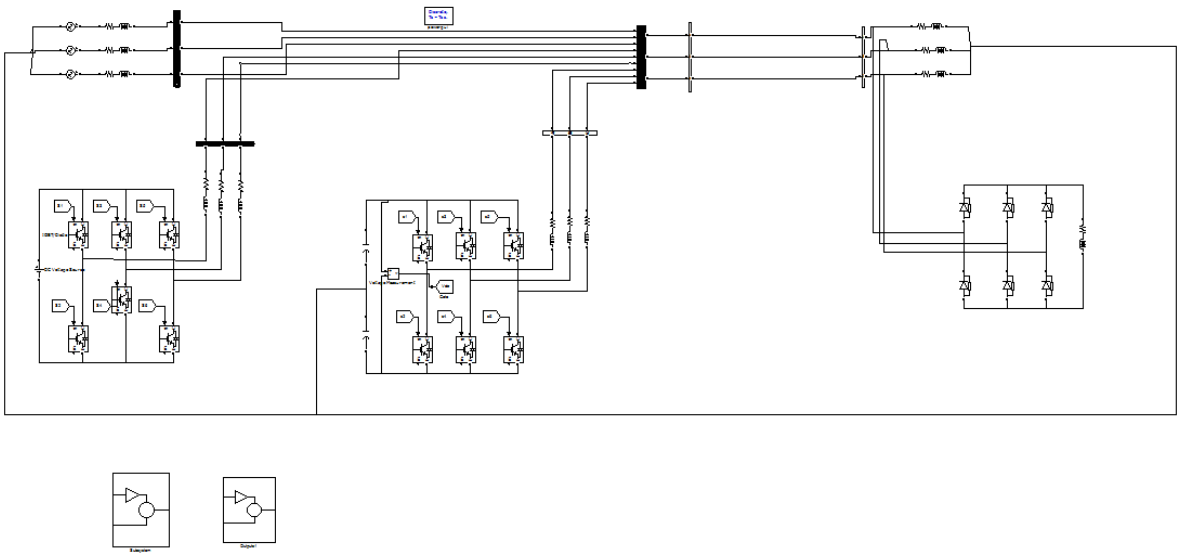

Figure 5: Simulink Model of DVSI Scheme

If these distorted voltages are used for the reference current generation of AVSI, the current compensation will not be proper [14]. Therefore, the fundamental positive sequence of voltages is extracted from these distorted voltages. The resonant controller design is explained in Section III-C. These voltages are further used for the generation of inverter reference currents.

Parameters	Values
Grid voltage	400V(L-L)
Fundamental frequency	50Hz
Feeder impedance	R_g =0.5Ω, L_g =1.0Mh
AVSI	c_1 = c_2 =2400μF V_{dcref} =1040V Interfacing inductor, L_{fx} =20mH Inductor resistance, R_{fx} =0.25Ω Hysteresis band $(\pm h_x)$=0.1A
MVSI	DC-link voltage. V_{dcm}=650V Interfacing inductor, L_{fm} =5mH Inductor resistance, R_{fm} =0.25Ω Hysteresis band $(\pm h_m)$=0.1A
Unbalanced linear loads	Z_{la} =35+j19Ω Z_{lb} =30+j15Ω Z_{lc}=23+j12Ω
Nonlinear loads	3ϕ diode bridge rectifier with DC side current of 3.0A
DC voltage controller gains	K_{Pv}=10, K_{Iv} =0.05

Table 1: System parameters for simulation study

Fig. 6(a)–(d) represents active power demanded by load (P_l), active power supplied by grid (P_g), active power supplied by MVSI ($P_{\mu g}$), and active power supplied by AVSI (P_x), respectively. It can be observed that, from t = 0.1 to 0.4 s, MVSI is generating 4 kW power and the load demand is 6 kW. Therefore, the remaining load active power (2 kW) is drawn from the grid. During this period, the micro grid is operating in grid sharing mode. At t = 0.4 s, the micro grid power is increased to 7 kW, which is more than the load demand of 6 kW. This micro grid power change is considered to show the change of operation of MVSI from grid sharing to inject to the grid and hence, the power drawn from grid is shown as negative.

Figure 6(a): Load Active Power

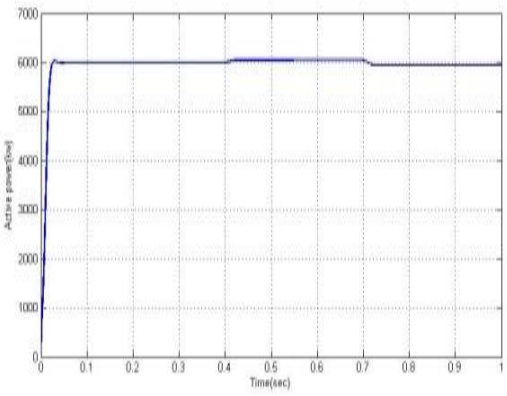

Figure 6(b): Active Power Supplied by grid

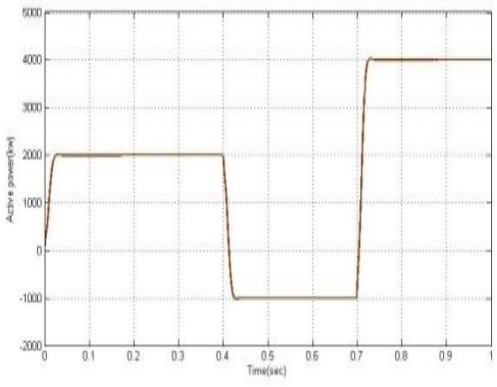

Figure 6(c): Active Power Supplied by MVSI, Figure 6(d): Active Power supplied by AVSI

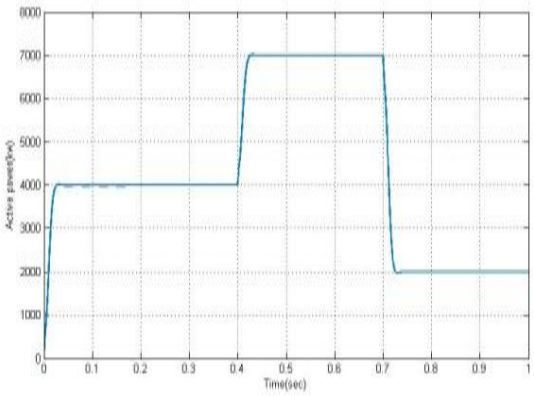

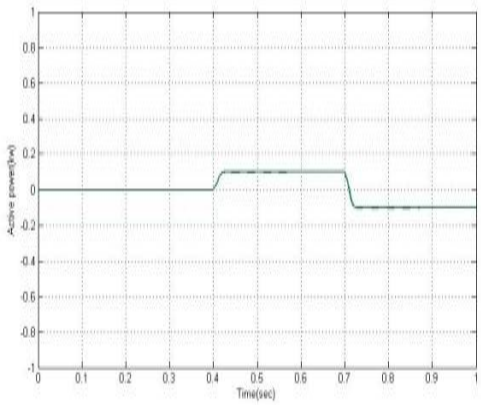

Figure 7(a)–(c) shows the load reactive power (Q_l), reactive power supplied by AVSI (Q_x), and reactive power supplied by MVSI ($Q_{\mu x}$), respectively. It shows that total load reactive power is supplied by AVSI, as expected. Figure 8(a)–(d) shows the plots of load currents (i_{1abc}) currents drawn from grid (i_{gabc}), currents drawn from MVSI ($i_{\mu gabc}$) and currents drawn from the AVSI ($i_{\mu xabc}$) respectively. The load currents are unbalanced and distorted. The MVSI supplies balanced and sinusoidal currents during grid supporting and grid injecting modes. The currents drawn from grid are also perfectly balanced and sinusoidal, as the auxiliary inverter compensates the unbalance and harmonics in load currents.

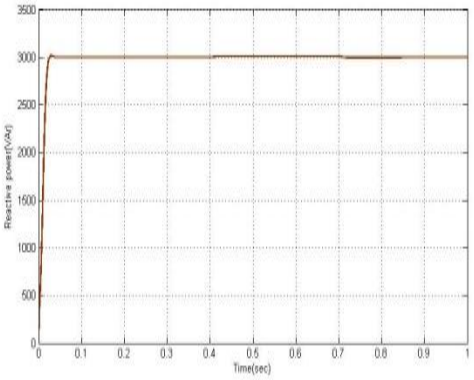

Figure 7(a): Load Reactive Power

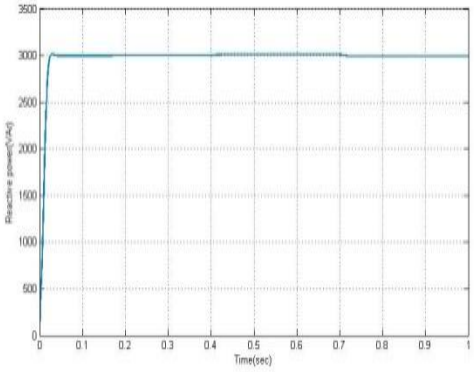

Figure 7(b): Reactive Power Supplied by AVSI

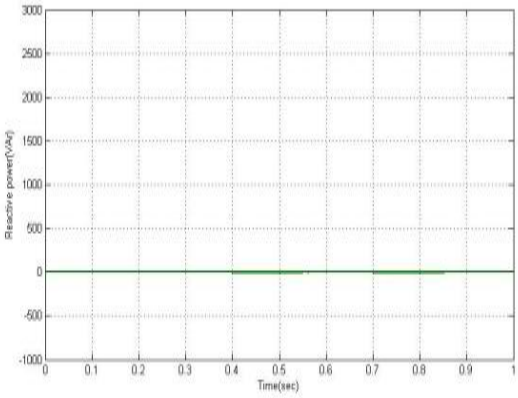

Figure 7(c): Reactive Power Supplied by MVSI

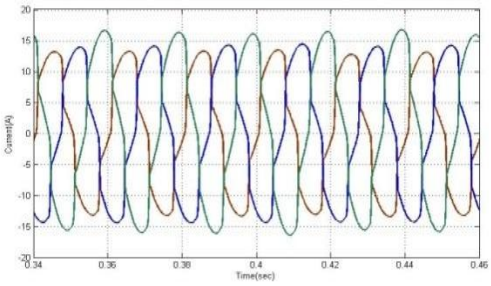

Figure 8(a): Load Currents

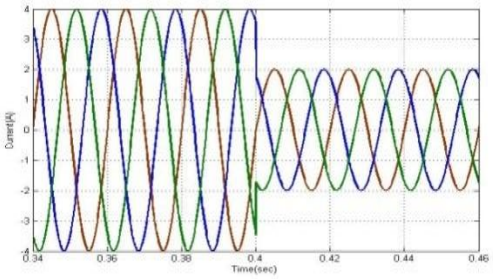

Figure 8(b): Grid Currents

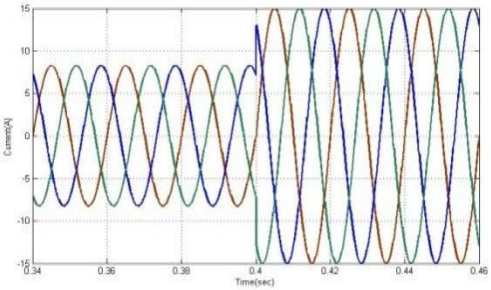

Figure 8(c): MVSI Currents

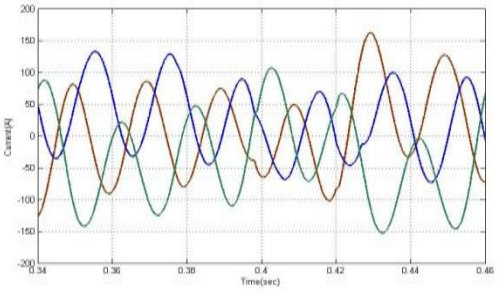

Figure 8(d): AVSI Currents

Figure 9(a) shows the plot of fundamental positive sequence of PCC voltage (V_{ta1}^{+}) and grid current in phase-a (i_{ga}) during grid sharing and grid injecting modes. During grid sharing mode, this PCC voltage and grid current are in phase and during grid injecting mode, they are out of phase. Figure 9(b) establishes that MVSI current in phase-a is always in phase with fundamental positive sequence of phase-a PCC voltage. The same is true for other two phases. Thus the compensation capability of AVSI makes the source current and MVSI current at unity power factor operation. Figure 10(a), (b) and Figure 11(a), (b) shows grid voltages and load voltages with conventional PI and PI+RC Controller respectively.

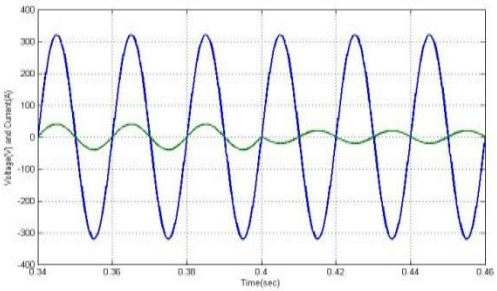

Figure 9(a): PCC voltage and grid current (phase-a)

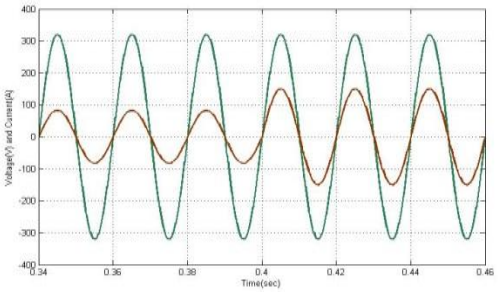

Figure 9(b): PCC voltage & MVSI current (phase-a)

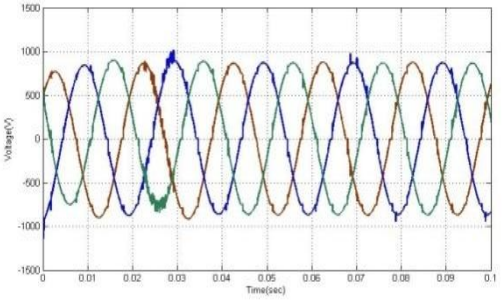

Figure 10(a): Grid voltages with Conventional PI controller

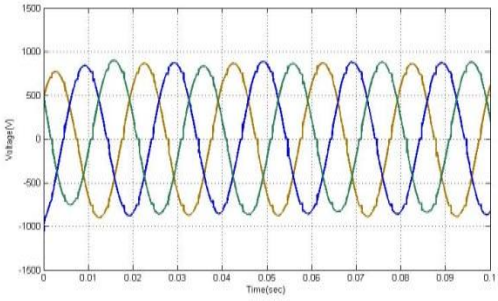

Figure 10(b): Grid voltages with proposed PI+ RC controller

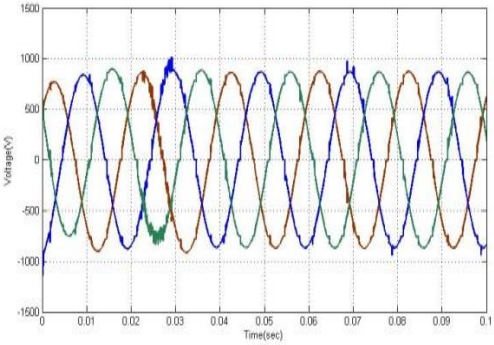

Figure 11(a): Load Voltages with conventional PI controller

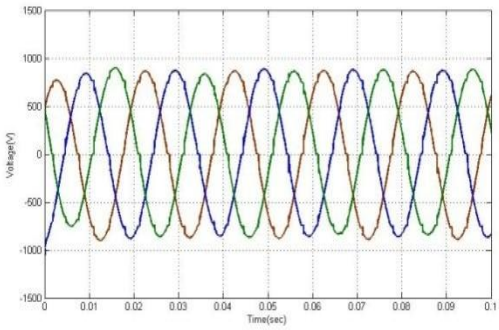

Figure 11(b): Load Voltages with proposed PI + RC controller

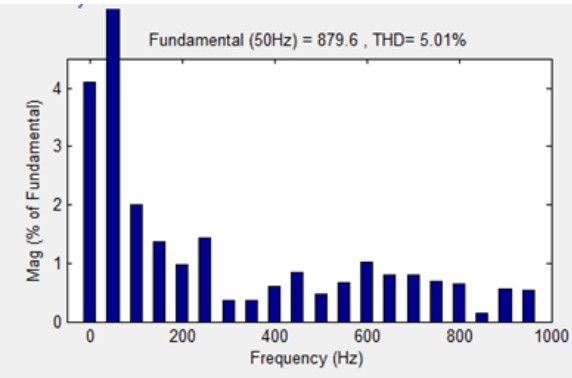

Figure 12(a): THD of Grid voltages with Conventional PI controller

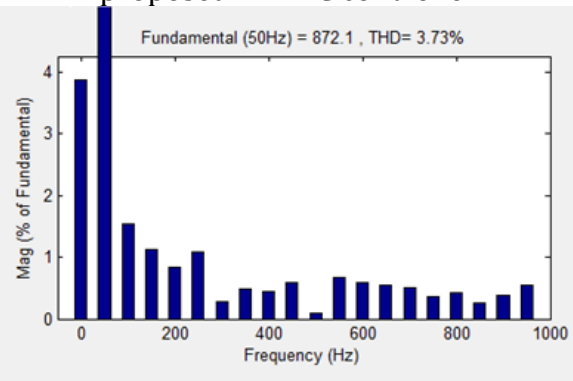

Figure 12(b): THD of Grid voltages with proposed PI+RC controller

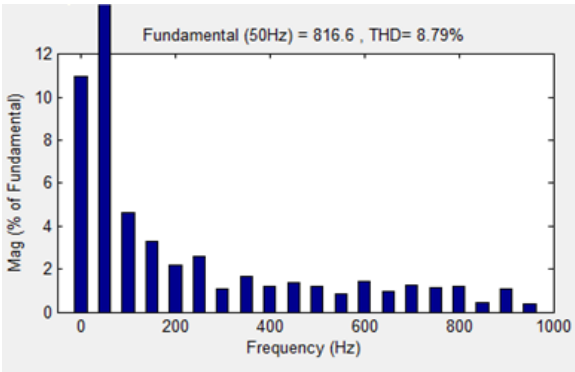

Figure 13(a): THD of load voltages with conventional PI controller

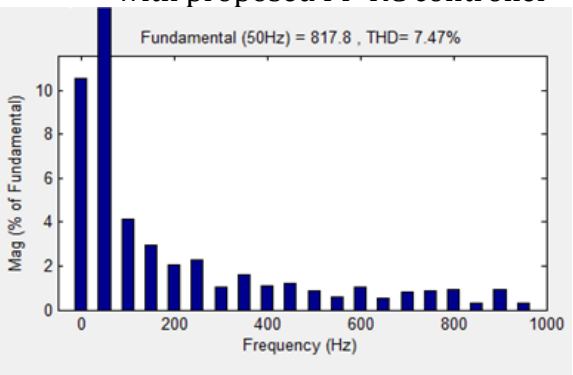

Figure 13(b): THD of load voltages with proposed PI+RC controller

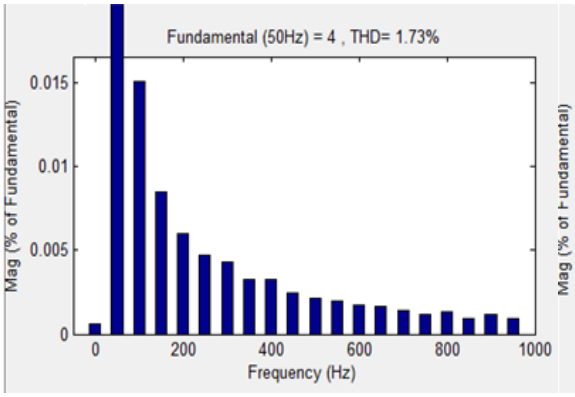

Figure 14(a): THD of Grid current with conventional PI controller

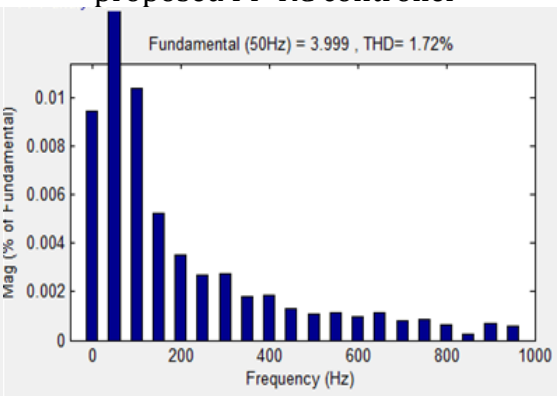

Figure 14(b): THD of Grid current with proposed PI+RC controller

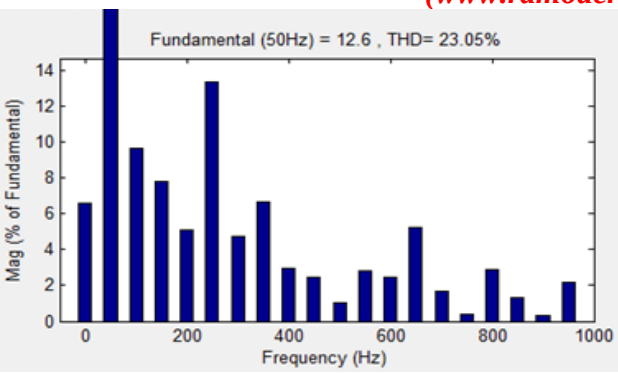

Figure 15(a): THD of load current with conventional PI controller

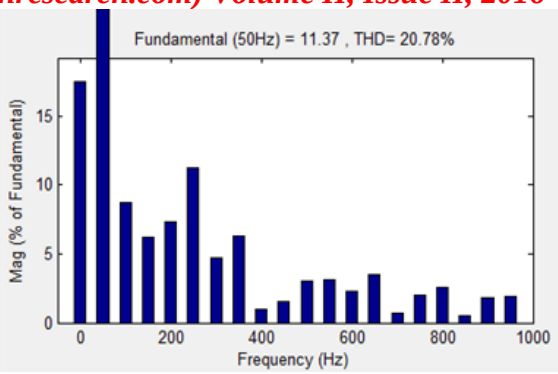

Figure 15(b): THD of load current with proposed PI+RC controller

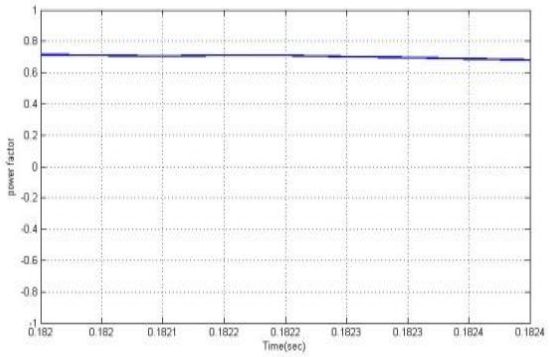

Figure 16(a): Power factor = 0.78 with conventional PI controller

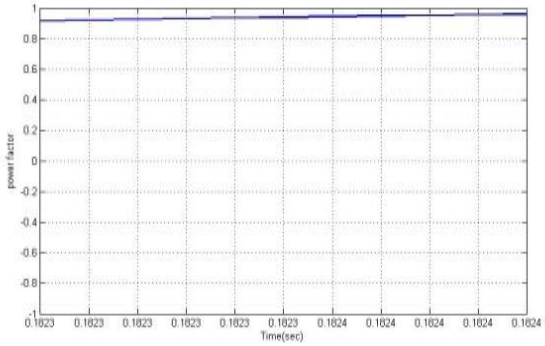

Figure 16(b): Power factor = 0.93 with proposed PI+RC controller

System Parameters	PI Controller	PI+RC Controller
Grid Voltage(THD)	5.01 %	3.73 %
Load Voltage(THD)	8.79 %	7.47 %
Grid Current(THD)	1.73 %	1.72%
Load Current(THD)	23.05%	20.78%
Frequency(Hz)	49.96Hz	49.99Hz
Power Factor	0.78	0.93

Table 2: Comparison of results

5. Conclusion:

A DVSI scheme is proposed for micro grid systems with improve the power quality. The modified controller has the capability to exchange power from distributed generators (DGs) and also to compensate the local unbalanced and nonlinear load. The performance of the proposed scheme has been validated through simulation studies. As compared to a single inverter with multifunctional capabilities, a DVSI has many advantages such as, increased reliability, lower cost due to the reduction in filter size, and more utilization of inverter capacity to inject real power from DGs to micro grid. DVSI with PI + Resonant Controller with PWM current controller has less number of components, more power quality is obtained with low THD percentage as tabulated in Table 2, grid frequency variation from 49.96Hz to 49.99Hz and power factor from 0.78 to 0.93 from conventional PI to proposed PI+RC controller respectively.

6. References:

1. A. Kahrobaeian and Y.-R. Mohamed, “Interactive distributed generation interface for flexible micro-grid operation in smart distribution systems,” IEEE Trans. Sustain. Energy, vol. 3, no. 2, pp. 295–305, Apr. 2012.

2. X. Yu and A. Khambadkone, "Reliability analysis and cost optimization of parallel-inverter system," IEEE Trans. Ind. Electron., vol. 59, no. 10, pp.3881–3889, Oct. 2012.
3. N. R. Tummuru, M. K. Mishra, and S. Srinivas, "Multifunctional VSC controlled micro grid using instantaneous symmetrical components the-ory," IEEE Trans. Sustain. Energy, vol. 5, no. 1, pp. 313–322, Jan. 2014.
4. S. Iyer, A. Ghosh, and A. Joshi, "Inverter topologies for DSTATCOM applications—A simulation study," Electr. Power Syst. Res., vol. 75, no. 23, pp. 161–170, 2005.
5. A. Ghosh and A. Joshi, "A new approach to load balancing and power factor correction in power distribution system," IEEE Trans. Power Del., vol. 15, no. 1, pp. 417–422, Jan. 2000.
6. U. Rao, M. K. Mishra, and A. Ghosh, "Control strategies for load compensation using instantaneous symmetrical component theory under different supply voltages," IEEE Trans. Power Del., vol. 23, no. 4,
2310–2317, Oct. 2008.
7. A. Ghosh and G. Ledwich, "Load compensating DSTATCOM in weak AC systems," IEEE Trans. Power Del., vol. 18, no. 4, pp. 1302–1309, Oct. 2003.
8. R. Majumder, A. Ghosh, G. Ledwich, and F. Zare, "Load sharing and power quality enhanced operation of a distributed micro grid," IET Renewable Power Gener., vol. 3, no. 2, pp. 109–119, Jun. 2009.
9. M. Prodanovic and T. Green, "Control and filter design of three-phase inverters for high power quality grid connection," IEEE Trans. Power Electron., vol. 18, no. 1, pp. 373–380, Jan. 2003.
10. M. Singh, V. Khadkikar, A. Chandra, and R. Varma, "Grid interconnection of renewable energy sources at the distribution level with power-quality improvement features," IEEE Trans. Power Del., vol. 26, no. 1, pp. 307–315, Jan. 2011.
11. M. K. Mishra and K. Karthikeyan, "Design and analysis of voltage source inverter for active compensators to compensate unbalanced and non-linear loads," in Proc. IEEE Int. Power Eng. Conf., 2007, pp. 649–654.